Rhinology, 43, 115-120, 2005

The analysis of anterior skull base from two different perspectives: coronal and reconstructed sagittal computed tomography*

Osman Kursat Arikan[1], Birsen Unal[2], Mustafa Kazkayasi[1], Can Koc[1]

[1] Department of Otorhinolaryngology - Head and Neck Surgery, Kirikkale University, Kirikkale, Turkey
[2] Department of Radiology, School of Medicine, Kirikkale University, Kirikkale, Turkey

SUMMARY

The aim of the study was to determine the heights of the anterior skull base and the distances between the anterior nasal spine and the skull base at three levels by means of coronal and reformatted sagittal images of computed tomography. The present study was performed on coronal and reformatted sagittal CT scans of 30 patients with sinonasal complaints. On the coronal view, the heights of the cribriform plate, the roof of ethmoid, and lateral lamella and the medial take-off angle between the ethmoid roof and cribriform plate were measured at different levels. On the reformatted sagittal images the distances from the nasal spine to the anterior cranial base at three different levels were measured. Then, the side-to-side variability of these measurements was statistically compared. The variations with normal distribution and abnormal distribution were analysed by paired t test and Wilcoxon paired-signed rank test, respectively. A statistically significant difference was detected only between the right and left sides in the height of the lateral lamella at the crista galli level ($p<0.05$). The lateral lamella at the crista galli level on the left side was higher than on the right side. No statistically significant differences between the left and the right sides were noted in the heights and the distances of other data ($p>0.05$). The normal anatomy of the anterior skull base has been described in detail on coronal and reconstructed sagittal computed tomography. These measurements may be helpful in the presurgical evaluation of patients undergoing endoscopic sinus surgery to optimize surgical safety.

Key words: anterior skull base, computed tomography, ethmoid roof, cribriform plate, sagittal reconstruction

INTRODUCTION

The ethmoid bone consists of four parts: the perpendicular plate, the cribriform plates (horizontal laminas), and two labyrinths. The cribriform plates form two linear depressions in the inferior portion of the anterior cranial fossa. Laterally, the cribriform plate articulates with the ethmoidal process of the frontal bone, which forms the roof of the ethmoid. The medial aspect of the ethmoid roof articulates with the thin bone of the lateral lamella of the cribriform plate. It is important to remember that the morphometric anatomy of the ethmoid roof can vary widely [1, 2].

Intranasal surgery of the paranasal sinus has gained significant improvements as a result of the introduction of endoscopes. Although great progress has been achieved in endoscopic sinus surgery (ESS), many surgeons remain hesitant to perform a complete ethmoidectomy. Because the bones adjacent to the anterior skull base are as thin as the septa in the ethmoid sinus, surgeons tend to lose their orientation in this area, especially in nasal polyposis and in revisions [3]. Inadvertent violation of the cribriform plate or ethmoid roof may result in intracranial injury, cerebrospinal fluid rhinorrhea and a consequent increased risk of developing meningitis [4]. To avoid these complications, a detailed knowledge of the anterior skull base anatomy of the patient is crucial. Because of the variations and complexity of the paranasal sinus anatomy, this has to be assessed on a patient to patient basis [5]. This is usually determined using preoperative computed tomographic (CT) imaging of the paranasal sinuses. CT is of special interest to the endoscopic sinus surgeon for planning surgery as it allows detailed imaging of the nasal passages, paranasal sinuses, and the adjacent structures.

In previous studies, using CT, heights of the cribriform plate and the ethmoid roof were only measured at one level [6-8]. Since the skull base has a decline as the sections proceed posteriorly, it seems logical to perform these measurements at more than one level. Thus, we conducted a prospective review of coronal CT scans, performed on patients with sinonasal symptoms, to measure the heights of the cribriform plate and

*Received for publication: April 26, 2004; accepted: October 18, 2004

the ethmoid roof at three levels. In addition, the distance from the nasal spine to the anterior cranial base, the plane of surgical approach, was measured at three levels by the use of reconstructed sagittal computed tomography images.

MATERIALS AND METHODS

Patients

Forty-two consecutive patients who presented with complaints related to the nose and paranasal sinuses were prospectively evaluated by CT at our institution from January 2003 through December 2003. Patients' age, sex, and working diagnosis at the time of the imaging were recorded. The primary reasons for obtaining a CT scan in these subjects were recurrent acute sinusitis, chronic sinusitis, nasal polyposis or the 'sinus-type' headaches or facial pain. Only adults over 18 years of age were included. Previous paranasal sinus surgery, malignant disease involving the anterior cranial fossa, mucocele, or nasal polyps that obscured analysis of the subtle anatomic features were excluded from the study. Consequently, 30 scans that met our criteria constituted the basis for our trial. All scans were interpreted by the same radiologist (BU) and otolaryngologist (OKA) with consensus.

CT scan

Routine CT examination was performed on the coronal plane with 3-mm slice thickness and no interslice gap, at 120kV and 85 mAs, starting from the anterior border of the frontal sinus to the anterior clinoid process (Elscint, SeleCT, Israel). From these images, 1 mm thickness coronal (exactly perpendicular to the hard palate), and 0.5-mm thickness sagittal oblique reconstructions were obtained. Sagittal oblique images were created as slices, passing medially from the inferior contour of the bony nasal septum and laterally from the ethmoid bulla with approximately 10^{o} craniocaudal angulation from the midsagittal line, on the right and the left sides separately (Figure 1). All the measurements were performed bilaterally on the screen of the CT console. On coronal reconstruction images, a horizontal line from the most inferior contour of nasal fossa was drawn. Perpendicular lines from the ethmoid roof to this horizontal line, at the midlevel between the midsagittal line and lamina papyracea, and also from the cribriform plate to the same horizontal line were drawn (Figure 2). The heights of the ethmoid roof and the cribriform plate were measured at 3 different coronal planes, passing from crista galli, ethmoid bulla, and sphenoethmoid junction. The height of the lateral lamella between the medial aspect of ethmoid roof and cribriform plate was also measured at the level of crista galli and bulla ethmoidalis (Figure 3). Again on reconstructed coronal images, the take-off angle of the ethmoid roof from the horizontal was measured at the level of crista galli (Figure 4). On reconstructed sagittal images, the anterior nasal spine was set as focus point and lines connecting this point with anterior cranial base at the levels of nasofrontal recess, ethmoid bulla, and the sphenoethmoid junction were drawn (Figure 5). On these lines the distances between the focus point and anterior cranial base were measured and recorded.

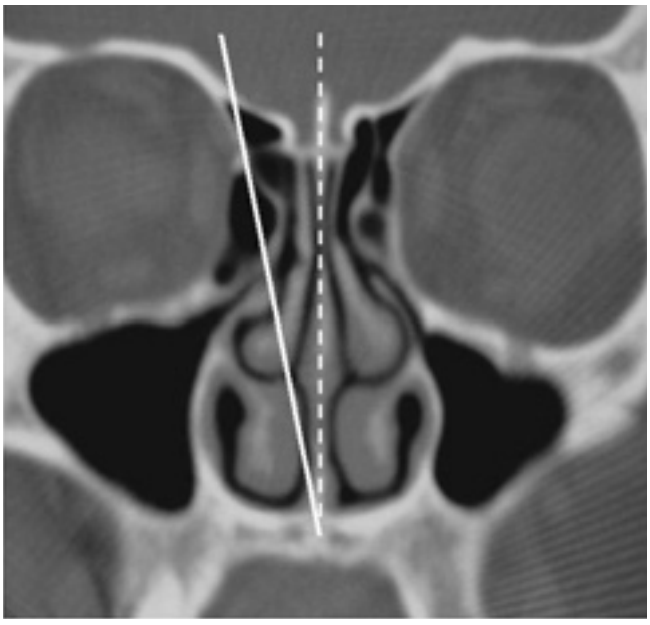

Figure 1. A coronal computed tomography scan through the bulla ethmoidalis. The white line represents the plane that we obtained through sagittal reconstruction.

Statistical Analysis

We statistically compared the side-to-side variability of these measurements. The Shapiro Wilk test was performed to determine whether the variables were normally distributed or not. The abnormally distributed variables which were the distances from hard palate to cribriform plate at the bulla ethmoidalis and the junction of sphenoethmoid levels were analyzed by the Wilcoxon paired-signed rank test. Since the other data had parametric distributional properties, a paired t test was performed.

All statistical analyses were performed through SPSS (For Windows, version 11.0, Chicago, IL, USA). Differences were considered significant when the p-value was less than 0.05.

RESULTS

The ages of the patients ranged from 18 to 64 years, with an average age of 37.5 years. Sixteen of the patients were female and 14 were male.

Irrespective of the sides, the measurements were as follows: 1) the height of cribriform plate relative to the hard palate (mean ± SD) at crista galli, bulla ethmoidalis and the junction of sphenoethmoid levels were 46.95 ± 3.36, 46.04 ± 4.24 and 48.66 ± 4.35 mm respectively, 2) the distance between the ethmoid roof and hard palate (mean ± SD) at crista galli, bulla ethmoidalis and the junction of sphenoethmoid levels were 53.11 ± 4.65, 51.58 ± 5.39 and 49.05 ± 4.44 mm respectively, 3) the distance from the nasal spine to the skull base (mean ± SD) at nasofrontal recess, bulla ethmoidalis and the junction of sphenoethmoid levels were 64.76 ± 9.17, 59.78 ± 5.73 and 64.16 ±

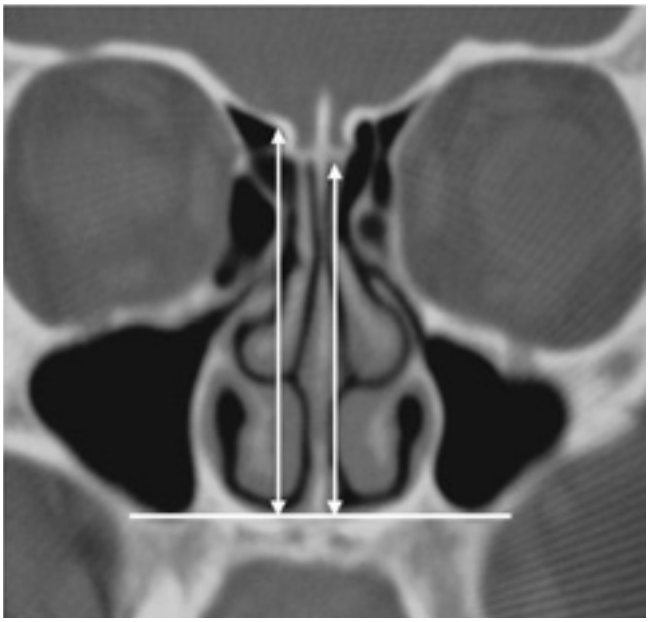

Figure 2. The measurements of the cribriform plate and the roof of ethmoid on coronal computed tomography.

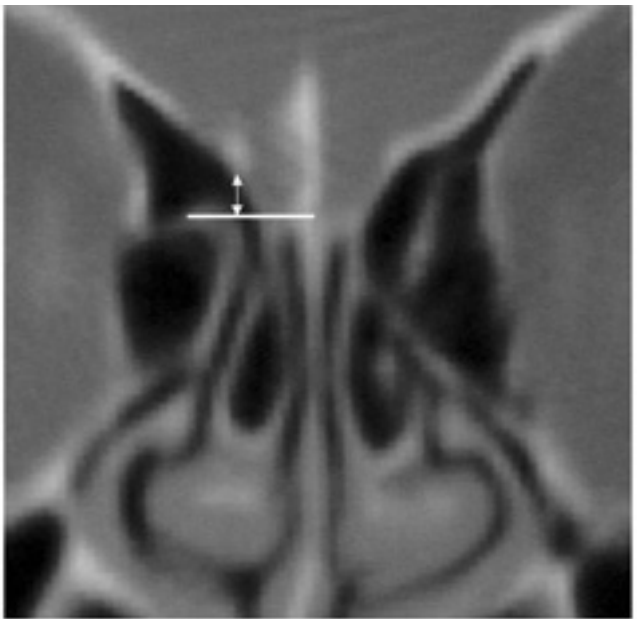

Figure 3. The measurement of the lateral lamella on coronal computed tomography.

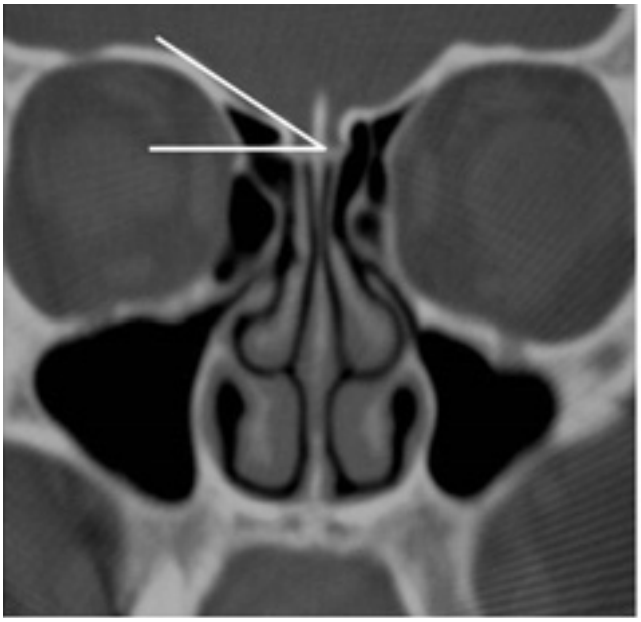

Figure 4. The measurement of the take-off angle of the ethmoid roof from the horizontal on coronal computed tomography.

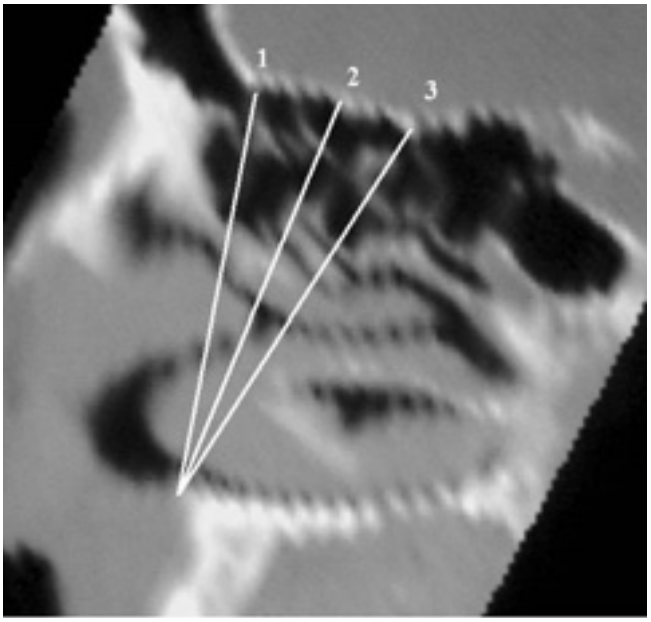

Figure 5. The measurements between the anterior nasal spine and skull base on reformatted sagittal images.

5.75 mm respectively, and 4) the take-off angle (mean ± SD) was $33.86^{o} \pm 8.10^{o}$. The results of the measurements have been presented in Table 1.

A statistically significant difference was found between the right and left sides in the height of the lateral lamella at the nasofrontal recess level ($p<0.05$). The lateral lamella at the crista galli level on the left side was higher than on the right side. No statistically significant differences between the left and the right sides were demonstrated in the heights and the distances of other data. The statistical comparison of right- and left-sided measurements have been summarized in Tables 2 and 3.

DISCUSSION

The shape of the anterior cranial base greatly varies among individuals. In this trial, the measurements of the anterior cranial base were obtained from two different perspectives: coronal and sagittal. To our knowledge, no study describing the anterior cranial base as defined in this study has been conducted to date.

A great number of studies have analyzed the ethmoid roof [6-9]. The height of the nasal cavity in different parts was investigated both in dried bone and, when covered by mucosa, on

Table 1. The results of the measurements.

	Level	Mean	SD	Median	Minimum	Maximum
HP→ER (mm)	Crista Galli	53.11	4.65	53.55	44.10	62.65
	Bulla ethmoidalis	51.58	5.39	51.38	40.45	65.95
	Sphenoethmoid junction	49.05	4.44	48.25	40.80	59.75
HP→CP (mm)	Crista galli	46.95	3.36	46.98	40.15	56.55
	Bulla ethmoidalis	46.04	4.24	46.23	38.45	57.80
	Sphenoethmoid junction	48.66	4.35	48.05	40.80	59.75
Height of LL (mm)	Crista Galli	3,60	1,09	3,68	1,05	6,95
	Bulla ethmoidalis	2,92	1,07	3,05	1,15	4,70
ANS →ASB(mm)	Nasofrontal recess	64,76	9,17	65,93	49,10	85,00
	Bulla ethmoidalis	59,78	5,73	59,83	49,25	77,90
	Sphenoethoid junction	64,16	5,75	65,38	52,55	76,10
Take-off Angle (°)	Crista galli	33,86	8,10	32,50	12,50	47,00

HP→ER: The distance from hard palate to ethmoid roof
HP→CP: The distance from hard palate to cribriform plate
ANS→ASB: The distance between anterior nasal spine and anterior skull base
LL: Lateral lamella
SD: Standard deviation

Table 2. Statistical evaluation of normally distributed variables.

	Level	Right		Left			
		Mean	SD	Mean	SD	t	P
HP → ER (mm)	Crista Galli	53.16	4.93	53.06	4.54	0.268	0.791
	Bulla ethmoidalis	51.30	5.56	51.85	5.42	-1.405	0.171
	Sphenoethmoid junction	48.92	4.40	49.18	4.59	-0.976	0.337
HP → CP (mm)	Crista galli	46.93	3.73	46.97	3.33	1.475	0.151
Height of LL (mm)	Crista galli	3.41	1.13	3.77	1.20	-2.298	0.029
	Bulla ethmoidalis	3.11	1.33	2.73	1.05	1.894	0.068
ANS →ASB(mm)	Nasofrontal recess	63.86	9.92	65.65	9.28	-1.712	0.098
	Bulla ethmoidalis	59.24	5.56	60.32	6.48	-1.554	0.131
	Sphenoethmoid junction	64.08	6.08	64.23	6.31	-0.178	0.860
Take-off Angle (°)	Crista Galli	34.32	7.89	33.39	10.17	0.592	0.559

HP → ER: The distance from hard palate to ethmoid roof
HP → CP: The distance from hard palate to cribriform plate
ANS → ASB The distance between anterior nasal spine and anterior skull base
LL: Lateral lamella
SD: Standard deviation

Table 3. Statistical evaluation of abnormally distributed variables.

	Level	Right		Left			
		Median	Min-Max	Median	Min-Max	z	p
HP→CP (mm)	Bulla ethmoidalis	46.45	38.4-58.7	45.88	38.5-56.9	1.35	0.176
	Anterior wall of sphenoid sinus	48.31	39.4-60.4	49.00	42.2-59.9	1.23	0.216

HP→CP: The distance from hard palate to cribriform plate

human adult skulls [9,10]. The distance measured between the floor of the nasal cavity without a mucosal covering and the cribriform plate at the level of crista galli and bulla ethmoidalis was 49.11 (38-56) and 45.73 mm (38-52), respectively [9]. In our study, the median value of these lengths were 46.98 (40-57) and 46.23 (38-58) mm, respectively. Despite being based on CT, the measurements of this study were compatible with the results of Lang and Baumeister's report [9], with a few exceptions. Lebowitz et al. [7] retrospectively examined the coronal paranasal CT of 200 patients with suspected sinus disease for the height of the ethmoid roof. They found an asymmetry in 19 patients (9.5%). However, this difference between the left and right sides was not statistically significant. Similarly, Jones et al. [8] did not find any statistical differences between the right and left sides for the heights of the cribriform plate and ethmoid roof and also for the take–off angle of the ethmoid roof. Except the statistical difference for the height of the lateral lamella at the crista galli level between the sides, our results were consistent with two former studies. Although no statistically significant difference between left and right sides was demonstrable for the heights of anterior cranial base, intrasubject variation between the sides should be kept in mind.

The endocranial side of the cribriform plate forms the base of the fossa olfactoria, where the olfactory bulb is lodged. Therefore, the cribriform plate is at a lower level than the ethmoid roof, which flanks it [5]. The anterior part of the ethmoid roof lies more superior than the posterior part does, since the anterior cranial base descends 15 degrees from a horizontal plane as it passes posteriorly [11]. The reciprocal arrangement between the cribriform plate and the roof of ethmoid sinus was investigated by Keros [12] who distinguished different types based on the different levels: type 1 with 1-3 mm difference; type 2 with 4-7 mm difference; and type 3 in which the cribriform plate is located 8-16 mm below the ethmoid roof. These variations are taken into account when planning or performing surgery, because the greater the difference, the stronger the relationship between the ethmoidal cells and the endocranium [13]. The distance between the ethmoid roof and cribriform plate can be evaluated easily on coronal scans. The heights measured between the cribriform plate and the highest point of the ethmoid roof were 6.9 (2-18) mm in the anterior third, and 5.8 (2-18) mm in the posterior third [14]. In our study, the differences in height between these two structures at the crista galli, bulla ethmoidalis, and the junction of sphenoethmoid levels were 6.16, 5.54, and 0.39 mm, respectively. It was noticed that the difference in distance between the ethmoid roof and cribriform plate sharply decreased from the level of the crista galli to the sphenoid sinus. Moreover, the two halves of the cribriform plate are positioned at distinctly different heights in 80% of the cases [14]; the mean height of the right half at the level of the crista galli and sphenoethmoid junction in our study were lower than on the left by 0.04 and 0.69 mm, respectively. In contrast, the cribriform plate at the bulla ethmoidalis level on the right side was higher than on the left by 0.32 mm. Prior to sinus surgery, surgeons need to be aware of a declining level of the skull base and different heights of the cribriform plate between the sides.

Common structures of the lateral nasal wall can be easily identified on sagittal views [15]. In particular, the important anteroposterior course of the skull base can be sufficiently demonstrated. Sagittal CT scans allow measurements of the distances from the nasal spine to the anterior skull base. These measurements, which may improve the precision and safety of FESS, become critical during endonasal sinus surgery.
May et al. [16] reported that the distance and the angles from the anterior nasal spine to the middle of the roof of the ethmoid sinus, ethmoid-sphneoid sinus junction and the anterior face of the sphenoid sinus can be measured with great accuracy on lateral plain roentgenographs. The averages of values for the distances from the nasal spine to the skull base at the level of midfovea and sphenoethmoid junction were 6.2 and 6.9 cm, respectively [17]. Due to superimposition, it is not possible to distinguish between the sides on plain radiographic images. Unlike May's study, we used reformatted sagittal CT that could provide more details than plain radiography. On reformatted sagittal images, the mean distances from the nasal spine to the skull base at the nasofrontal recess, bulla ethmoidalis and the junction of sphenoethmoid levels were 64.76, 59.78 and 64.16 mm, respectively. On sagittal scans, the distances between the nasal spine and the cranial base were greater on the left than on the right. However, it was found that the difference for each of the levels between the left and right sides was not statistically significant.

This study aimed to provide surgeons with a detailed analysis of anterior cranial base based on coronal and reconstructed sagittal CT, which can help improve surgical results and reduce complication rates.

REFERENCES

1. Chakeres DW (1985) Computed tomography of the ethmoid sinuses. Otolaryngol Clin North Am 18: 29-42.
2. Davis WE, Tempter J, Parsons DS (1996) Anatomy of the paranasal sinuses. Otolaryngol Clin North Am 29: 57-74.
3. Kim SS, Lee JG, Kim KS, Kim HU, Chung IH, Yoon JH (2001) Computed tomographic and anatomical analysis of the basal lamellas in the ethmoid sinus. Laryngoscope 111: 424-429.
4. Cumberworth BL, Sudderick RM, Mackay IS (1994) Major complications of functional endoscopic sinus surgery. Clin Otolaryngol 19: 248-253.
5. Teatini G, Simonetti G, Salvolini U, et al (1987) Computed tomography of the ethmoid labyrinth and adjacent structures. Ann Otol Rhinol Laryngol 96: 239-250.
6. Dessi P, Moulin G, Triglia JM, Zanaret M, Cannoni M (1994) Difference in the height of the right and left ethmoidal roofs: a possible risk factor for ethmoidal surgery. Prospective study of 150 CT scans. J Laryngol Otol 108: 261-262.
7. Lebowitz RA, Terk A, Jacobs JB, Holliday RA (2001) Asymmetry of the ethmoid roof: analysis using coronal computed tomography. Laryngoscope 111: 2122-2124.
8. Jones TM, Almadhi JMD, Bhalla RK, Lewis-Jones H, Swift AC

(2002) The radiological anatomy of the anterior skull base. Clin Otolaryngol 27: 101-105.
9. Lang J, Baumeister R (1982) Postnatal growth of the nasal cavity. Gegenbaurs Morph Jb 128: 354-393.
10. Lang J, Sakals E (1981) The height of the cavitas nasi, the length of the bony palate, and the size and arrangement of the conchae nasales and apertura sinus sphenoidalis. Anat Anz 149: 297-318.
11. Hosemann WG, Weber RK, Keerl RE, Lund VJ (2000) Minimally invasive endonasal sinus surgery. Georg Thieme Verlag Publishers, Stuttgart, Germany, pp. 9.
12. Keros P (1962) On the practical value of differences in the level of the lamina cribrosa of the ethmoid. Z Laryngol Rhinol Otol 41: 808-813.
13. Kainz J, Stammberger H (1989) The roof of the anterior ethmoid: a place of least resistance in the skull base. Am J Rhinol 89: 191-199.
14. Lang J (1989) Clinical anatomy of the nose, nasal cavity and paranasal sinuses. Georg Thieme Verlag Publishers, Stuttgart, Germany, pp. 51-53.
15. Hilger AW, Ingels K, Joosten F (1999) Sagittal computed tomography reconstruction of the lateral nasal wall for functional endoscopic sinus surgery. Clin Otolaryngol 24: 527-530.
16. May M, Mester SJ, O'Daniel TG, Curtin HD (1990) Decreasing the risks of endonasal endoscopic nasal surgery by imaging techniques. Op Tech Otolaryngol Head Neck Surg 1: 89-91.
17. May M, Mester SJ, Levine HL (1993) Offive evaluation of nasosinus disorders: patient selection for endoscopic sinus surgery. In: Levine HL, May M (Eds.) Endoscopic Sinus Surgery. Thieme Medical Publishers, New York, USA, pp. 60-90.

Osman Kursat Arikan, MD
Kirikkale Universitesi Tip Fakultesi
Kulak Burun Bogaz Anabilim Dali
71100 Kirikkale
Turkey

Tel: +90-318-225-2485/ext.172
Fax: +90-318-225-2819
E-mail: osman.arikan@gediknet.com